Free Radical Research, February 2009; 43(2): 93–99

informa
healthcare

Alloxan-dialuric acid cycling: A complex redox mechanism

JANINA A. ROSSO, MARCOS A. ASTORGA, DANIEL O. MÁRTIRE, & MÓNICA C. GONZALEZ

Instituto de Investigaciones Fisicoquímicas Teóricas y Aplicadas (INIFTA), Departamento de Química, Facultad de Ciencias Exactas, Universidad Nacional de La Plata (UNLP). C.C. 16, Suc. 4, (1900) La Plata, Argentina

(Received 3 July 2008; revised 17 October 2008)

Abstract
Time-resolved kinetic studies involving the reactions of alloxan ($A.H_2O$) with the reducing species superoxide and carbon dioxide radical anions and the reaction of dialuric acid (HA^-) with sulphate radicals showed that the same radical ($AH^\bullet$) was formed either by the one-electron reduction of alloxan or by the one-electron oxidation of dialuric acid. A mechanism including several reversible reactions was proposed and validated. A detailed kinetic analysis yields the following bimolecular rate constants: $k(A.H_2O + SO_4^{\bullet -}) < 10^5$ M^{-1} s^{-1}, $k(A.H_2O + O_2^{\bullet -}) = (3.4 \pm 0.5) \times 10^6$ M^{-1} s^{-1}, $k(HA^- + SO_4^{\bullet -}) = (8 \pm 1) \times 10^7$ M^{-1} s^{-1} and $k(AH^\bullet + AH^\bullet) = (1.7 \pm 0.8) \times 10^8$ M^{-1} s^{-1}. From these values, the redox potentials $E^\circ(A.H_2O,H^+/AH^\bullet) = (-290 \pm 20)$ mV, $E^\circ(AH^\bullet/HA^-) = (277 \pm 20)$ mV and $E^\circ(A.H_2O,H^+/HA^-) = (-15 \pm 20)$ mV, were obtained.

Keywords: *Alloxan, dialuric acid, superoxide radical ions, sulphate radicals.*

Introduction

Alloxan causes diabetes in experimental animals through its ability to destroy the insulin-secreting β-cells of the pancreas. Since the discovery of alloxan-induced diabetes mellitus in animals [1] several researchers have discussed the mechanisms of its toxicity.

Alloxan is apparently selectively taken up by the GLUT-2 glucose transporter in the pancreatic β-cell membrane [2,3]. Nowadays, it is well established that a redox cycling involving alloxan and its reduced product dialuric acid initiates an intracellular generation of reactive oxygen species, ROS [4–6], mediated by physiological glutathione (GSH) and other thiols.

Alloxan is hydrophilic and chemically unstable. In aqueous solution, the monohydrated ($A.H_2O$) is the most stable form of alloxan. It is in acid-base equilibrium with deprotonated species with pK values of 6.6, 8.4 and 13.1 [7]. In neutral or alkaline solutions, alloxan suffers a rearrangement described as a 'benzilic acid rearrangement' to form alloxanic acid [5,7].

Alloxan is reactive toward thiols, undergoing redox cycling in the presence of GSH and oxidizing protein-bound thiol groups, as reflected by inhibition of the thiol enzymes, hexokinase and glucokinase. Alloxan is reduced by GSH via the alloxan radical into dialuric acid, which was detected by ESR spectroscopy [8], and autooxidizes back to alloxan. Formation of dialuric acid is reported to be an essential pre-requisite for any superoxide radical formation from alloxan under reducing conditions [9]. Moreover, alloxan itself is a scavenger of superoxide radical anions [9]. ROS formed during this redox cycling process are able to destroy -cells in islets of Langerhans. On the other hand, alloxan ability to initiate thiol oxidation promotes its interaction with biological structures and therefore disturbs biological functions expanding its cytotoxic action [6].

Correspondence: Janina A. Rosso, Instituto de Investigaciones Fisicoquímicas Teóricas y Aplicadas (INIFTA), C.C. 16, Suc. 4, (1900) La Plata, Argentina. Tel: 54-221-425 74 30. Fax: 54-221-425 46 42. Email: janina@inifta.unlp.edu.ar

ISSN 1071-5762 print/ISSN 1029-2470 online
DOI: 10.1080/10715760802616650

Reduction of alloxan, oxidation of GSH and formation of oxidized glutathione (GSSG) were continuously recorded in experiments conducted with different oxygen concentrations to evaluate the impact of oxygen on the redox cycling initiated by a given initial ratio of GSH and alloxan [5].

The alloxan radical may also be generated by reduction of alloxan by the hydrated electron (e_{aq}^-) or the carbon dioxide radical anion ($CO_2^{\bullet -}$). Disproportionation to dialuric acid and alloxan was the observed decay path of this radical in the continuous γ and pulse-radiolysis experiments [10,11].

Air-saturated aqueous solutions of dialuric acid are unstable because the oxidation of dialuric acid by molecular oxygen leads to alloxan formation [12]. Dialuric acid has a pK value of 2.8 [7] and its absorption spectrum has a maximum at 275 nm with $\varepsilon^{275} = 16\,000\ \text{M}^{-1}\ \text{cm}^{-1}$ [10].

Auto-oxidation of dialuric acid in the presence of oxygen to yield superoxide and hydrogen peroxide takes place even in the absence of a thiol [13]. The process involves the semiquinone type alloxan radical, which may be further oxidized by molecular oxygen to yield alloxan and superoxide [13]. Supported on the latter reactions it was suggested that intracellular superoxide dismutase provides transitory protection against the oxidation products of dialuric acid and a prolonged protection should only be achieved if accumulation of alloxan is also prevented.

Despite the abundant literature on the importance of alloxan-dialuric acid redox cycling in producing ROS, there is still confusion on the reactions involved in these processes. Therefore, we describe here our time-resolved kinetic experiments on the oxidation of dialuric acid by the strong one-electron oxidant sulphate radical ions ($SO_4^{\bullet -}$) and on the reduction of alloxan by the superoxide radical ions ($O_2^{\bullet -}$).

Materials and methods

Alloxan tetrahydrate (Fluka, UK), potassium formate (Carlo Erba p. a., Italy), K_2HPO_4 and KH_2PO_4 (Baker ACS, Mexico), $Na_2S_2O_8$, NaOH, and $HClO_4$ (Merck p.a. quality, Darmstadt, Germany) were used as received. Distilled water (>18 MΩ cm^{-1}, <20 ppb of organic carbon) was obtained from a Millipore (Bedford, MA) system. The absorption spectra of the samples were measured with a Cary 3 UV/VIS spectrophotometer or with a Heweltt Packard 8452A diode array spectrophotometer.

To avoid decomposition of the monohydrated ion of alloxan ($A.H_2O$) to alloxanic acid during the experiments, aqueous solutions of pH in the range 4–5 were used.

The spectra of alloxan solutions show an absorbance maximum at 275 nm which decreases with time upon saturation of the solutions with O_2 and is characteristic of the dialuric acid. Taking $\varepsilon^{275} = 16\,000\ \text{M}^{-1}\ \text{cm}^{-1}$ for the dialuric acid [10], the presence of 0.4% wt/wt of dialuric acid in freshly prepared solutions of the commercial batch of Alloxan tetrahydrate used is calculated. Dialuric acid was therefore eliminated from the mother solutions by bubbling oxygen until constant absorption at 275 nm.

Flash-photolysis experiments were carried out using a conventional equipment (Xenon Co. model 720C) with modified optics and electronics. Two co-linear quartz Xenon high-intensity pulsed flash tubes (Xenon Corp. P/N 890-1128, FWHM ≤ 20 μs), with a continuous spectral distribution ranging from 200–600 nm and maximum at ~ 450 nm were used. The analysis source was a high pressure mercury lamp (Osram HBO-100 W). The optical path length of the quartz sample cell (1 cm internal diameter) was 10 cm. The monochromator collecting the analysis beam (Bausch & Lomb, high intensity) was coupled to a photomultiplier (RCA 1P28) whose output signal was registered by a digital oscilloscope (Leader LBO-5825). Digital data were stored in a personal computer. To avoid product accumulation, each solution was irradiated only once. The temperature was measured inside the reactor cell with a calibrated Digital Celsius Pt-100 Ω thermometer.

The photolysis of peroxodisulphate, $S_2O_8^{2-}$, provides a clean source for sulphate radical anions ($SO_4^{\bullet -}$) with high pH-independent quantum yields [14]. These radicals efficiently react with formate ions to yield carbon dioxide radical anions ($CO_2^{\bullet -}$), which in the presence of molecular oxygen are quantitatively converted into $O_2^{\bullet -}$ [15].

Results and discussion

The possible oxidation of $A.H_2O$ by the strong one-electron oxidant sulphate radical anion ($SO_4^{\bullet -}$) was investigated by flash-photolysis of aqueous 5×10^{-3} M peroxodisulphate solutions in the presence and absence of $A.H_2O$.

Experiments performed in the absence of alloxan showed formation of a transient species in the wavelength range from 300–550 nm whose decay rate and spectrum are in agreement with those reported in the literature for $SO_4^{\bullet -}$ [14,16] and is, therefore, assigned to this species. The $SO_4^{\bullet -}$ radicals decay with simultaneous first and second order components due to reactions R2 and R3 in Table I with rate constants k_2 and k_3, respectively. The weight factor of each process strongly depends on the irradiation light intensity and peroxodisulphate concentration [14] and the absorbance traces were fitted to equation (1).

$$A(\lambda) = \frac{k_{first}}{b(\lambda) \times \exp(k_{first} \times t) - c(\lambda)} \quad (1)$$

Table I. Reaction mechanism proposed.

$S_2O_8^{2-} \xrightarrow{h\nu} SO_4^{\bullet -} + SO_4^{\bullet -}$		R1
$SO_4^{\bullet -} + S_2O_8^{2-}/H_2O \longrightarrow$	6×10^5 M^{-1} s^{-1} [31]	R2
$SO_4^{\bullet -} + SO_4^{\bullet -} \longrightarrow S_2O_8^{2-}$	2.25×10^8 M^{-1} s^{-1} [31]	R3
$SO_4^{\bullet -} + HCO_2^- \longrightarrow CO_2^{\bullet -} + SO_4^{2-} + H^+$	1.1×10^8 M^{-1} s^{-1} [15]	R4
$CO_2^{\bullet -} + CO_2^{\bullet -} \longrightarrow C_2O_4^{2-}$	1.25×10^8 M^{-1} s^{-1} [32]	R5
$CO_2^{\bullet -} + O_2 \longrightarrow O_2^{\bullet -} + CO_2$	4.0×10^9 M^{-1} s^{-1} [32]	R6
$HO_2^{\bullet} \leftrightharpoons O_2^{\bullet -} + H^+$	$K_a = 3.33 \times 10^{-5}$ [32]	R7
$O_2^{\bullet -} + HO_2^{\bullet} + H_2O \longrightarrow H_2O_2 + O_2 + HO^-$	5.0×10^7 M^{-1} s^{-1} [31]	R8
$HO_2^{\bullet} + HO_2^{\bullet} + H_2O \longrightarrow H_2O_2 + O_2$	2.0×10^6 M^{-1} s^{-1} [31]	R9
$HO_2^{\bullet} + H_2O_2 \longrightarrow HO^{\bullet} + H_2O + O_2$	530.0 [31]	R10
$A.H_2O + SO_4^{\bullet -} \longrightarrow$	$< 10^5$ M^{-1}s^{-1} [a]	R11
$A.H_2O + CO_2^{\bullet -} + H^+ \longrightarrow AH^{\bullet} + CO_2 + H_2O$	3.2×10^7 M^{-1} s^{-1} [10] [c]	R12
$A.H_2O + O_2^{\bullet -} + H^+ \longrightarrow AH^{\bullet} + O_2 + H_2O$	$(3.4 \pm 0.5) \times 10^6$ M^{-1} s^{-1} [a, d, e]	R13a
$A.H_2O + HO_2^{\bullet} \longrightarrow AH^{\bullet} + O_2 + H_2O$		R13b
$HA^- + O_2 \longrightarrow AH^{\bullet} + O_2^{\bullet -}$	(0.1–1.0) M^{-1} s^{-1} [b, d, e]	R14
$HA^- + SO_4^{\bullet -} \longrightarrow AH^{\bullet} + SO_4^{2-}$	$(8 \pm 1) \times 10^7$ M^{-1} s^{-1} [a]	R15
$HA^- + HO_2^{\bullet} + H^+ \longrightarrow AH^{\bullet} + H_2O_2$	$(1–7) \times 10^4$ M^{-1} s^{-1} [b]	R16
$AH^{\bullet} + AH^{\bullet} + H_2O \longrightarrow HA^- + A.H_2O + H^+$	$(1.7 \pm 0.8) \times 10^8$ M^{-1} s^{-1} [a, c, d]	R17
$HA^- + A.H_2O + H^+ \longrightarrow 2\ AH^{\bullet} + H_2O$	(0.05–0.10) M^{-1} s^{-1} [b]	R18
$AH^{\bullet} + O_2 + H_2O \longrightarrow A.H_2O + O_2^{\bullet -} + H^+$	$(6–8) \times 10^5$ M^{-1} s^{-1} [b]	R19

[a]This work.
[b]Optimized range of values obtained by computational simulation. The lower and upper limit values are those not affecting the goodness of the simulations.
[c]Other literature values from reference [11]: $k_{12} = 3.7 \times 10^7$ M^{-1} s^{-1} and $k_{17} = 1.6 \times 10^8$ M^{-1} s^{-1}
[d]Other literature values from reference [13]: $k_{13a} = 1 \times 10^5$ M^{-1} s^{-1}, $k_{14} = 0.5$ M^{-1} s^{-1}, $k_{16} = 1.5 \times 10^4$ M^{-1} s^{-1}, $k_{17} = 1 \times 10^8$ M^{-1} s^{-1}, $k_{18} = 45$ M^{-1} s^{-1}, $k_{19} = 3 \times 10^5$ M^{-1} s^{-1}.
[e]Other literature values from reference [21]: $k_{13a} = 5 \times 10^5$ M^{-1} s^{-1}, $k_{14} = 210$ M^{-1} s^{-1}, $k_{16} < 10^3$ M^{-1} s^{-1}, $k_{19} = 3.5 \times 10^7$ M^{-1} s^{-1}.

$A(\lambda)$ is the time- and wavelength-dependent absorbance, $c(\lambda) = 2\ k_3/\varepsilon(\lambda)l$ with $\varepsilon(\lambda)$ = absorption coefficient and l = optical pathlength and $b(\lambda) = c(\lambda) + k_{first}/A_o(\lambda)$ with $A_o(\lambda)$ the absorbance immediately after the lamp pulse. In the absence of added substrates, $k_{first} = k_2$.

No change was detected in the decay rate of $SO_4^{\bullet -}$ radical by addition of 8×10^{-4} M A.H_2O, which indicates that the oxidation of A.H_2O by sulphate radicals ($[SO_4^{\bullet -}]_0 \cong 2–3 \times 10^{-6}$ M), if occurs, should have a reaction rate constant lower than 10^5 M^{-1}s^{-1}, R11 in Table I.

Peroxodisulphate photolysis in Ar-saturated solutions containing formate yields $CO_2^{\bullet -}$ radical anions, reaction R4 [15], which were reported to reduce A.H_2O to $AH^{\bullet}$ radicals, R12 [11,17]. In the presence of molecular oxygen, $CO_2^{\bullet -}$ efficiently reacts with O_2 to yield superoxide radical anions, $O_2^{\bullet -}$, R6, which are also reported to reduce A.H_2O to $AH^{\bullet}$ radicals, R13a [18].

Flash-photolysis experiments with Ar-, air- or O_2-saturated 2×10^{-2} M $Na_2S_2O_8$ solutions containing 4×10^{-3} M HCO_2Na and different alloxan concentrations were performed to obtain information on the reaction paths generating and depleting $AH^{\bullet}$ radicals. Experiments performed with O_2-saturated solutions and [A.H_2O] $< 1 \times 10^{-3}$ M showed formation of a transient species identified as the superoxide radical ion, with decay rates increasing with the concentrations of alloxan. The decay of the traces taken at 290 nm (see Figure 1, inset) could be well fitted to a mixed first and second-order rate law with an equation similar to that shown in equation (1). Since $O_2^{\bullet -}$, in equilibrium with $HO_2^{\bullet}$, is the main species absorbing at 290 nm ($\varepsilon_{290\ nm}(O_2^{\bullet -}) = 570$ M^{-1} cm^{-1}), a value of $(2.1 \pm 0.1) \times 10^7$ M^{-1} s^{-1} for the apparent second order rate constant for the reaction of $O_2^{\bullet -}$ with $HO_2^{\bullet}$ as expected at pH 6 [19]. A plot of the pseudo first order rate constant, k_{first}, vs [A.H_2O], shown in Figure 1, yields an apparent rate constant (see equation (2)) $k_{13app} = (3.2 \pm 0.3) \times 10^6$ M^{-1} s^{-1} for the reduction of A.H_2O with $O_2^{\bullet -}$/$HO_2^{\bullet}$ radicals. This value is smaller than the rate constant reported for the reduction of A.H_2O with

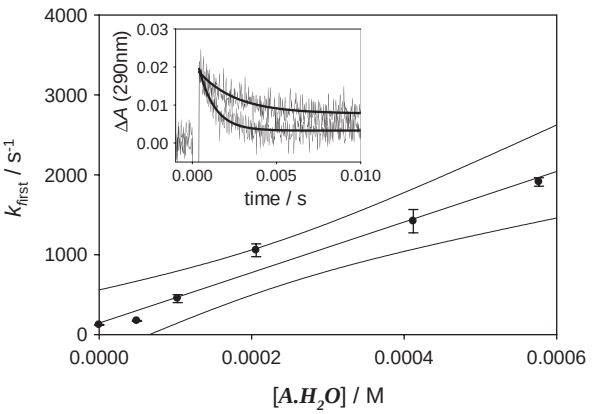

Figure 1. Plot of pseudo first order rate constant of the decay of $O_2^{\bullet -}$, k_{first}, vs A.H_2O concentration obtained in flash-photolysis experiments with air-saturated 2×10^{-2} M $Na_2S_2O_8$ solutions containing 4×10^{-3} M HCO_2Na. *Inset*: Traces taken at 290 nm for the experiments of the main figure obtained in the presence of 1.03×10^{-4} M A.H_2O (upper trace) and 2.06×10^{-4} M A.H_2O (lower trace).

the carbon dioxide radical anion ($k_{12} = 3.2 \times 10^7$ M^{-1} s^{-1} [10]).

$$k_{13app} = \frac{k_{13a} + k_{13b} \times \frac{[H^+]}{K_{a7}}}{1 + \frac{[H^+]}{K_{a7}}} \quad (2)$$

where k_{13a} and k_{13b} are the rate constants for the reactions of $A.H_2O$ with $O_2^{\bullet -}$ and $HO_2^{\bullet}$, respectively (R13*a* and R13*b* in Table I), and K_{a7} the acid-base equilibrium constant involving the $HO_2^{\bullet}/O_2^{\bullet -}$ radicals, R7.

Since the reduction of alloxan is taking place and that the reducing ability of the radicals follows the trend $CO_2^{\bullet -}$ ($E^\circ(CO_2/CO_2^{\bullet -}) = -1800$ mV) > $O_2^{\bullet -}$ ($E^\circ(O_2/O_2^{\bullet -}) = -330$ mV) > $HO_2^{\bullet}$ ($E^\circ(O_2, H^+/HO_2^{\bullet}) = -37$ mV) [20], we assume that $k_{12} > k_{13a} > k_{13b}$ and then the second term in the numerator of equation (2) could be neglected at pH = 6 and the value $k_{13a} = (3.4 \pm 0.5) \times 10^6$ M^{-1} s^{-1} is assigned to the reaction of $A.H_2O$ with $O_2^{\bullet -}$ radical. The difference with the reported rate constant, $k_{13app} = 5.0 \times 10^5$ M^{-1} s^{-1} at pH 5.7 [19], cannot be explained.

Experiments performed with Ar-, air- or O_2-saturated 2×10^{-2} M $Na_2S_2O_8$ solutions containing 4×10^{-3} M HCO_2Na and $A.H_2O$ concentrations higher than 6×10^{-4} M, show formation of a transient species with absorption maxima at ~310 and 360 nm, as shown in Figure 2 for air-saturated solutions. The transient absorption spectra is coincident with that reported for the $AH^{\bullet}$ radical, as expected from the one-electron reduction of $A.H_2O$ [4,11,17,21,22].

The decay of $AH^{\bullet}$ radicals in the absence of molecular oxygen may be well fitted to a second order law with $2k_{sec}/\varepsilon = 26\,500$ cm/s, see Figure 2.

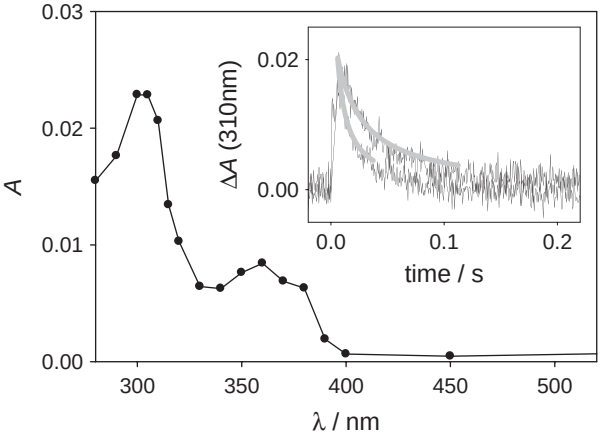

Figure 2. Transient absorption spectrum obtained at 10 ms after the flash irradiation of air-saturated 1.6×10^{-2} M $Na_2S_2O_8$ solutions containing 1.2×10^{-2} M HCOONa and 8×10^{-4} M $A.H_2O$. *Inset*: Traces taken at 310 nm for the experiments with Ar and oxygen-saturated solutions (upper and lower trace, respectively). The solid line corresponds to simulations.

Taking $\varepsilon_{AH^{\bullet}}$ (310 nm) = 4900 m^{-1} cm^{-1} [10], the rate constant for the disproportionation of $AH^{\bullet}$ radicals to yield HA^- and $A.H_2O$, R17, $k_{17} = (1.8 \pm 0.5) \times 10^8$ M^{-1} s^{-1} is obtained in agreement with reported values [4,10].

The decay of $AH^{\bullet}$ in experiments with air- or O_2-saturated solutions may be well fitted to a mixed first and second order law with $k_{sec} = (1.8 \pm 0.5) \times 10^8$ M^{-1} s^{-1}, in agreement with the observed rate constant for R17. The rate constant for the first order component depends on the dissolved oxygen concentration, as expected from reaction R19. Values of (22 ± 3) s^{-1} and (35 ± 3) s^{-1} were obtained for the first order decay rate constants in air- and O_2-saturated solutions, respectively.

The oxidation of dialuric acid by sulphate radicals was investigated by flash photolysis of freshly prepared Ar-bubbled solutions of Alloxan tetrahydrate containing 0.4% wt/wt of dialuric acid and sodium peroxodisulphate in the pH range 4–7 (H_2A/HA^-, $pK_a = 2.8$ [7]), where the main species of the substrate is HA^-.

Photolysis experiments of $Na_2S_2O_8$ solutions in the presence of $[HA^-] < 2 \times 10^{-5}$ M showed formation of transient species which were assigned to $SO_4^{\bullet -}$ radicals because of their transient spectrum [23]. The absorption traces showed faster decay kinetics with increasing concentration of HA^- and could be well fitted to a first order law with an apparent rate constant, k_{app} (see Figure 3). The slope of the linear plot of k_{app} vs $[HA^-]$ (Figure 3, inset) yields $k_{15} = (8 \pm 1) \times 10^7$ M^{-1} s^{-1}, on the order of the reported bimolecular rate constants for the reaction between HA^- and the hydroxyl radical [4].

Flash photolysis experiments with Ar-saturated 1×10^{-2} M $Na_2S_2O_8$ solutions containing 2.5×10^{-5} M HA^- show the fast depletion of sulphate radicals and subsequent formation of $AH^{\bullet}$ radical, whose decay may be well fitted to a second order rate

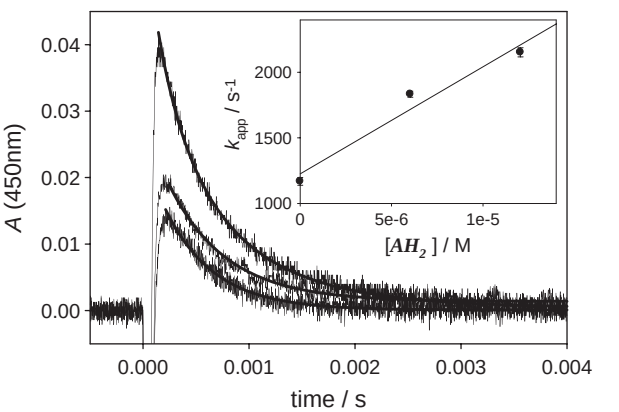

Figure 3. $SO_4^{\bullet -}$ radicals absorption traces at 450 nm obtained in flash photolysis experiments of 1×10^{-2} M $Na_2S_2O_8$ solutions containing: 0 m (upper trace); 6×10^{-6} M; and 1.2×10^{-5} M HA^- (lower trace). *Inset*: Dependence of the apparent rate constant k_{app} on the molar concentration of HA^-.

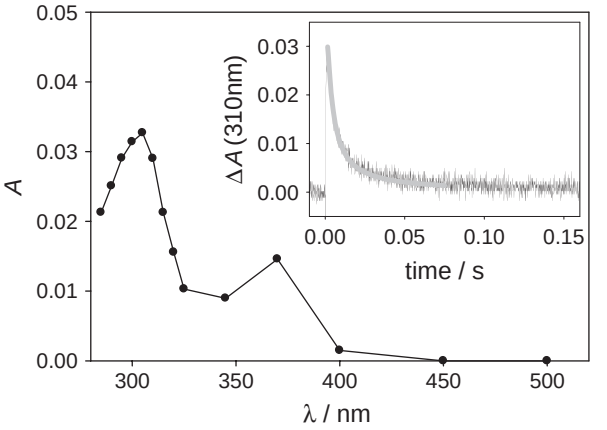

Figure 4. Transient absorption spectrum obtained at 1 ms after the flash irradiation of air-saturated 1.6×10^{-2} M $Na_2S_2O_8$ solutions containing 2.5×10^{-5} M HA^- and 4×10^{-3} M $A.H_2O$. *Inset*: Trace taken at 310 nm for the experiment of the main figure. The solid line corresponds to simulation.

law. Formation of this radical is expected from the one-electron oxidation of HA^- by $SO_4^{\bullet -}$ radicals, $E^\circ(SO_4^{\bullet -}/SO_4^{2-}) = 2.5$–$3.1$ V vs NHE [20].

Flash photolysis experiments performed with freshly prepared solutions but in the presence of molecular oxygen lead to the same intermediate, $AH^\bullet$ radical (see Figure 4). The observed radical decays in the presence of molecular oxygen following a mixed first and a second-order rate law, in agreement with our previous observations.

$AH^\bullet$ radicals are formed either by the one-electron reduction of $A.H_2O$ or by the one- electron oxidation of HA^-. The decay rate of the traces of $AH^\bullet$ radicals depends on the experimental conditions, such as the presence of molecular oxygen and $O_2^{\bullet -}/HO_2^\bullet$ radicals, and the initial $AH^\bullet$ radical concentration.

A simple kinetic analysis of the traces was not possible, so we attempted to reproduce the traces by numerical simulation, according to the kinetic scheme given in Table I (R2–R19).

The proposed reaction scheme considers $AH^\bullet$ radical oxidation to $A.H_2O$ with molecular oxygen, R19, and reaction R18, which is the reverse of the disproportionation, R17. This reaction is introduced to account for the oxidation of HA^- to $A.H_2O$ by molecular oxygen, which is auto-catalysed by generation of $A.H_2O$ [13]. A direct reaction between HA^- and oxygen should be of much lesser significance since it is expected to be extremely slow because it is spin restricted. The equilibrium condition for $O_2^{\bullet -}/HO_2^\bullet$ radicals was assumed.

The oxidation of $AH^\bullet$ radicals by $HO_2^\bullet$ to yield $A.H_2O$ and hydrogen peroxide [21,22] and reduction of $AH^\bullet$ radicals by $O_2^{\bullet -}$ to yield HA^- and molecular oxygen were not included because under our experimental conditions, the simulation of the absorbance traces are not sensitive to the presence of these reactions.

The simulation programme used the rate constants available in the literature and those found in the present work for reactions R13a, R15 and R17 as initial guesses. Only those rate constants not experimentally measured were allowed to vary (k_{14}, k_{16}, k_{18} and k_{19}) until a good agreement between simulated and experimental traces is obtained for different initial values of: $[O_2]$, $[A.H_2O]$, $[HA^-]$ and either $[SO_4^{\bullet -}]$ or $[CO_2^{\bullet -}]$. The goodness of the simulations are shown by the solid lines in Figure 2 (Inset) for experiments performed with Ar and oxygen-saturated solutions 1.6×10^{-2} M $Na_2S_2O_8$ solutions containing 1.2×10^{-2} M HCO_2Na and 8×10^{-4} M $A.H_2O$ and in Figure 4 (Inset) for air-saturated 1.6×10^{-2} M $Na_2S_2O_8$ solutions containing 2.5×10^{-5} M HA^- and 4×10^{-3} M $A.H_2O$.

Table I also includes literature data for the rate constants. For k_{14}, k_{16} and k_{19} there is good concordance between our values and these reported in Winterbourn et al. [13]. However, literature values for k_{13a} and k_{18} do not lead to an agreement between our simulated and experimental traces.

The one-electron reduction potentials of the redox pairs $E^\circ(A.H_2O,H^+/AH^\bullet)$ and $E^\circ(AH^\bullet/HA^-)$ may be calculated from the equilibrium constants of the reversible redox reactions involving them. The equilibrium constants K and the electromotive force of the galvanic cell, ΔE°, of the reversible reactions R13a and R19, R17 and R18, are shown in Table II, as Eq. I and Eq. II, respectively. Taking $E^\circ(O_2/O_2^{\bullet -}) = -330$ mV [20], $E^\circ(A.H_2O,H^+/AH^\bullet) = -290 \pm 20$ mV and $E^\circ(AH^\bullet/HA^-) = 277 \pm 30$ mV are obtained. From these values, $E^\circ(A.H_2O,H^+/HA^-) = -15 \pm 20$ mV is obtained for the two-electron reduction of alloxan to dialuric acid is.

Table II. Reduction potentials of the redox pairs involved in alloxan - dialuric acid cycle.

Equilibrium	K	ΔE° (mV)	Obtained value (mV)	
$A.H_2O + O_2^{\bullet -} + H^+ \leftrightharpoons AH^\bullet + O_2 + H_2O$ $\Delta E^\circ = E^\circ(A.H_2O,H^+/AH^\bullet) - E^\circ(O_2/O_2^{\bullet -})$	5.1 ± 1.5	40 ± 10 *	$E^\circ(A.H_2O,H^+/AH^\bullet) = -290 \pm 20$	Eq. I
$AH^\bullet + AH^\bullet + H_2O \leftrightharpoons HA^- + A.H_2O + H^+$ $\Delta E^\circ = E^\circ(AH^\bullet/HA^-) - E^\circ(A.H_2O,H^+/AH^\bullet)$	$(4.5 \pm 1.5) \times 10^9$	565 ± 15	$E^\circ(AH^\bullet/HA^-) = 277 \pm 30$	Eq. II
$A.H_2O + 2\,e^- + H^+ \longrightarrow HA^- + H_2O$ $E^\circ = E^\circ(A.H_2O,H^+/AH^\bullet) + E^\circ(AH^\bullet/HA^-)$			$E^\circ(A.H_2O,H^+/HA^-) = -15 \pm 20$	

*Taking $E^\circ(O_2/O_2^{\bullet -}) = -330$ mV [20].

Conclusion

The time-resolved kinetic studies involving the reactions of alloxan with superoxide and carbon dioxide radical anions and the reaction of dialuric acid with sulphate radicals allowed us to propose and validate a reaction mechanism. From the equilibrium constants of some involved reactions, the redox potentials for the couples $A.H_2O/AH^{\bullet}$ and $AH^{\bullet}/HA^{-}$ were calculated (see Table II).

The reversibility of the reactions involving $A.H_2O/AH^{\bullet}/HA^{-}$ in the presence of molecular oxygen resembles that reported for some quinone (Q)/semiquinone ($Q^{\bullet -}$)/hydroquinone (QH_2) systems. In fact, semiquinones reversibly react with O_2 to yield superoxide and the quinone, and hydroquinones react with $HO_2^{\bullet}$ to yield hydrogen peroxide and $Q^{\bullet -}$ [24–26]. Similarly, we here propose the reversible one-electron oxidations of $AH^{\bullet}$ to yield alloxan (R19 and R13a) and of HA^{-} to yield $AH^{\bullet}$ (R14 and R21).

Alloxan and dialuric acid act as a redox couple driven by reduced glutathione (GSH) or L-cysteine, generating in the presence of oxygen, both $O_2^{\bullet -}$ and $HO_2^{\bullet}$ [5,9]. The GSH-dependent formation of dialuric acid from alloxan is reported to be a decisive pre-condition for the subsequent ROS generation [9]. Alloxan is suggested to oxidize GSH to GSSG [27] via the alloxan radical [5]. During this redox cycling process, two molecules of GSH are oxidized to one molecule of GSSG and during each cycle one molecule of oxygen is simultaneously reduced to one molecule of hydrogen peroxide [5].

Formation of $AH^{\bullet}$ through GSH reduction of $A.H_2O$ requires one electron. Therefore, it is reasonable to assume that GSH is also one-electron oxidized in a first reaction step [28]. Taking $E^{\circ\prime}(GS^{\bullet},H^{+}/GSH) = 920 \pm 30$ mV [29] and $E^{\circ\prime}(A.H_2O/AH^{\bullet}) = -711 \pm 30$ mV at pH 7.4 (as calculated from the Nernst equation and the normal value in Table II), the reaction of GSH with alloxan to yield $AH^{\bullet}$ and $GS^{\bullet}$ is predicted to be thermodynamically not feasible under physiological conditions and formation of the $GS^{\bullet}$ radical seems to be precluded. However, a two electron reduction of $A.H_2O$ to AH^{-} by GSH seems thermodynamically favourable, as $E^{\circ\prime}(GSSG/2GSH) = -240$ mV [30] and $E^{\circ\prime}(A.H_2O,H^{+}/HA^{-}) = -236 \pm 30$ mV at pH 7 and 25°C. Therefore, an initial non-radical two-electron alloxan reduction to dialuric acid, followed by either R16 or the less efficient reactions R14 and R18 to yield $AH^{\bullet}$, is in complete agreement with the reported observation that the presence of dialuric acid is required for superoxide radical formation [9] and with GSH oxidation to GSSG. The SOD inhibition of the efficient $O_2^{\bullet -}$ oxidation of AH^{-} to $AH^{\bullet}$ radical, reaction R16, prevents alloxan regeneration through reaction R19 and therefore stops the GSH/alloxan auto-catalytic cycling.

Acknowledgements

This research was supported by PICT 2006-00876 Agencia Nacional de Promoción Científica y Tecnológica, Argentina (ANPCyT). M.C.G. and J.A.R. are research members of Consejo Nacional de Investigaciones Científicas y Técnicas (CONICET). D.O.M. is a research member of Comisión de Investigaciones Científicas de la Provincia de Buenos Aires (CIC).

***Declaration of interest*:** The authors report no conflicts of interest. The authors alone are responsible for the content and writing of the paper.

References

[1] Dunn JS, Sheehan HL, McLetchie NGB. Necrosis of the islets of Langerhans produced experimentally. Lancet 1943;241:484–487.

[2] Munday R, Ludwig K, Lenzen S. The relationship between the physicochemical properties and the biological effects of alloxan and several N-alkyl substituted alloxan derivatives. J Endocrinol 1993;139:153–163.

[3] Elsner M, Gurgul-Convey E, Lenzen S. Relation between triketone structure, generation of reactive oxygen species and selective toxicity of diabetogenic agent alloxan. Antioxid Redox Signal 2008;10:691–700. doi:10.1089/ars.2007.1816.

[4] Czerwińska M, Sikora A, Szajerski P, Adamus J, Marcinek A, Gebicki J, Bednarek P. Mechanistic aspects of alloxan diabetogenic activity: a key role of keto-enol inversion of dialuric acid on ionization. J Phys Chem A 2006;110:7272–7278,

[5] Brömme HJ, Weinandy R, Peschke E. Influence of oxygen concentration on redox cycling of alloxan and dialuric acid. Horm Metab Res 2005;37:729–733.

[6] Elsner M, Gurgul-Convey E, Lenzen S. Relative importance of cellular uptake and reactive oxygen species for the toxicity of alloxan and dialuric acid to insulin-producing cells. Free Radic Biol Med 2006;41:825–834.

[7] Kwart H, Sarasohn IM. Studies on the mechanism of the benzilic acid rearrangement; the rearrangement of alloxan (I). J Am Chem Soc 1961;83:909–919.

[8] Reif DW, Samokyszyn VM, Miller DM, Aust SD. Alloxan- and glutathione-dependent ferritin iron release and lipid peroxidation. Arch Biochem Biophys 1989;269:407–414.

[9] Brömme HJ, Eberlt H, Peschke D, Peschke E. Alloxan acts as prooxidant only under reducing conditions: influence of melatonin. Cell Mol Life Sci 1999;55:487–493.

[10] Houée-Levin C, Gardès-Albert M, Ferradini C, Pucheault J. Pulse radiolytic investigations of the redox system alloxan-dialuric acid: Evidence for a radical intermediate. Biochem Biophys Res Comm 1979;91:1196–1200.

[11] Houée-Levin C, Gardès-Albert M, Ferradini C, Pucheault J. Radiolysis study of the alloxan-dialuric acid couple. I. The reduction of alloxan by e_{aq}^{-} and $^{\bullet}COO^{-}$ radicals. Radiat Res 1980;83:270–278.

[12] Patterson JW, Lazarow A, Levey S. Alloxan and dialuric acid: their stabilities and ultraviolet absorption spectra. J Biol Chem 1949;177:187–196.

[13] Winterbourn CC, Cowden WB, Sutton HC. Auto-oxidation of dialuric acid, divicine and isouramil superoxide dependent

and independent mechanisms. Biochem Pharmacol 1989;38:611–618.
[14] McElroy WJ, Waygood SJ. Kinetics of the reactions of $SO_4^{\bullet -}$ radicals with $SO_4^{\bullet -}$, $S_2O_8^{2-}$ and Fe^{+2}. J Chem Soc Faraday Trans 1990;86:2557–2564.
[15] Rosso JA, Bertollotti SG, Braun AM, Mártire DO, Gonzalez MC. Reactions of carbon dioxide radical anion with substituted benzenes. J Phys Org Chem 2001;14:300–309.
[16] Choure SC, Bamatraf MMM, Rao BSM, Das R, Mohan H, Mittal JP. Hydroxylation of chlorotoluenes and cresols: a pulse radiolysis, laser flash photolysis, and product analysis study. J Phys Chem A 1997;101:9837–9845.
[17] Dohrmann JK, Livingston R, Zeldes H. Paramagnetic resonance study of liquids during photolysis. XII. Alloxan, parabanic acid and related compounds. J Am Chem Soc 1971;93:3343–3349.
[18] Bielski BHJ, Cabelli DE, Arudi RL, Ross AB. Reactivity of HO_2/O_2^- radicals in aqueous solution. J Phys Chem Ref Data 1985;14:1041–1100.
[19] Bielski BHJ, Cabelli DE. Superoxide and hydroxyl radical chemistry in aqueous solution. In: Foote CS, Valentine JS, Greenberg A, Liebman JF, editors. Active oxygen in chemistry. London: Chapman and Hall; 1995. p 66–104.
[20] Wardman P. Reduction potentials of one-electron couples involving free radicals in aqueous solution. J Phys Chem Ref Data 1989;18:1637–1755.
[21] Houée-Levin C, Gardes-Albert M, Ferrandini C, Pucheault J. Radiolysis study of the alloxan-dialuric acid couple. II. The autooxidation of dialuric acid. Radiat Res 1981;88:20–28.
[22] Houée C, Gardès M, Pucheault J, Ferradini C. Radical chemistry of alloxan-dialuric acid: role of superoxide radical. Bull Euro Physiopath Resp 1981;17(suppl):43–48.
[23] Rosso JA, Allegretti P, Mártire DO, Gonzalez MC. Reaction of sulphate and phosphate radicals with α, α, α-trifluorotoluene. J Chem Soc Perkin Trans 1999;2:205–210.

This paper was first published online on iFirst on 23 December 2008.

[24] Kalyanaraman B, Korytowski W, Pilas B, Sarna T, Land EJ, Truscott TG. Reaction between ortho-semiquinones and oxygen: pulse radiolysis, electron spin resonance, and oxygen uptake studies. Arch Biochem Biophys 1988;266:277–284.
[25] Patel KB, Willson RL. Semiquinone free radicals and oxygen pulse radiolysis study of one electron transfer equilibria. J Chem Soc Faraday Trans I 1973;69:814–821.
[26] Roginsky VA, Pisarenko LM, Bors W, Michel C. The kinetics and thermodynamics of quinine-semiquinone-hydroquinone systems under physiological conditions. J Chem Soc Perkin Trans 1999;2:871–876.
[27] Brömme HJ, Weinandy R, Peschke D, Peschke E. Simultaneous quantitative determination of alloxan, GSH and GSSG by HPLC. Estimation of the frequency of redox cycling between alloxan and dialuric acid. Horm Metab Res 2001;33:106–109.
[28] Winterbourn CC, Munday R. Glutathione-mediated redox cycling of alloxan. Biochem Pharm 1989;28:271–277.
[29] Madej E, Wardman P. The oxidizing power of the glutathione thiyl radical as measured by its electrode potential at physiological pH. Arch Biochem Biophys 2007;462:94–102.
[30] Shen D, Dalton TP, Nebert DW, Shertzer HG. Glutathione redox state regulates mitochondrial reactive oxygen production. J Biol Chem 2005;280:25305–25312.
[31] Neta P, Huie RE, Ross AB. Rate constants for reactions of inorganic radicals in aqueous solution. J Phys Chem Ref Data 1988;17:1027–1284.
[32] David Gara PM, Bucharsky E, Wörner M, Braun AM, Mártire DO, Gonzalez MC. Trichloroacetic acid dehalogenation by reductive radicals. Inorg Chim Acta 2007;360:1209–1216.